

Swimming sheet near a plane surfactant-laden interface

Vaseem A. Shaik and Arezoo M. Ardekani*

School of Mechanical Engineering, Purdue University, West Lafayette, Indiana 47907, USA



(Received 3 August 2018; revised manuscript received 10 December 2018; published 1 March 2019)

In this work we analyze the velocity of a swimming sheet near a plane surfactant-laden interface by assuming the Reynolds number and the sheet's deformation to be small. We observe a nonmonotonic dependence of the sheet's velocity on the Marangoni number (Ma) and the surface Péclet number (Pe_s). For a sheet passing only transverse waves, the swimming velocity increases with an increase in Ma for any fixed Pe_s . When Pe_s is increasing, on the other hand, the swimming velocity of the same sheet either increases (at large Ma) or it initially increases and then decreases (at small Ma). This dependence of the swimming velocity on Ma and Pe_s is altered if the sheet is passing longitudinal waves in addition to the transverse waves along its surface.

DOI: [10.1103/PhysRevE.99.033101](https://doi.org/10.1103/PhysRevE.99.033101)

I. INTRODUCTION

Our world is filled with motile microorganisms—*Helicobacter pylori* in stomach, *Escherichia coli* in intestines, *Chlamydomonas* in oceans and snow, *Paramecium* in stagnant basins and ponds, etc. Understanding the motion of these organisms in complex flow conditions is essential for addressing several biophysical questions [1]. One such complex bacterial motion is concerned with its locomotion near an interface which has applications in the biofilm formation and bioremediation of an oil spill. Researchers working on this topic have successfully explained (i) how the swimming speed of an organism gets altered near an interface [2–5], (ii) why these organisms move in circles near a plane interface [6,7], and (iii) why they reorient and get attracted toward an interface [8–11]. Recent works have also analyzed the change in the bacterial dynamics near an interface due to the (i) interface deformation [12–14], (ii) finite inertia of the swimmer or fluid [15,16], (iii) non-Newtonian suspending fluid [17–19], and (iv) presence of surfactants [9–11].

We briefly review the works on locomotion near a surfactant covered interface. Near a plane surfactant-laden interface, the attraction and reorientation of a swimming microorganism is similar to its behavior near a plane wall but its circling direction can be opposite to the one near a clean interface [9]. Considering the trapping of marine microbes onto drops, it was reported that the trapping dynamics outside drops is similar to that outside a rigid sphere, but the surfactant-laden drops have better trapping characteristics than a rigid sphere or a clean drop [11]. This is nonintuitive as a surfactant-laden drop usually has characteristics that are intermediate between a rigid sphere and a clean drop. Analogous to the interface deformations, finite inertia of the fluid or the organism and the non-Newtonian rheology of the fluid, the surfactant redistribution can enable a time-reversible swimming microorganism near an interface to achieve a net motion [20].

These works on the locomotion near a surfactant-laden interface assumed the surfactant to be either incompressible

(valid at large Marangoni numbers Ma , ratio of Marangoni stresses to the bulk viscous stresses) [21–23] or compressible [24] but its surface advection being negligible compared to its surface diffusion (valid at small surface Péclet numbers Pe_s , ratio of surface advection to the surface diffusion of the surfactant). The objective of this work is to analyze the locomotion near a surfactant-laden interface for all values of surface Péclet and Marangoni numbers.

To model the surfactant as generally as possible without losing the analytical tractability, we use a simple model microorganism. Hence, we model the organism as a two-dimensional (2D) infinitely long swimming sheet that propels by propagating waves along its surface. This model was first proposed by Taylor [25] who considered a sheet passing transverse waves to represent a monoflagellated organism such as spermatozoon. It was later extended by Blake [26] who allowed the passage of both longitudinal and transverse waves along the sheet to represent the almost flat ciliated organisms such as *Paramecium* or *Opalina*. Due to the mathematical simplicity associated with this model, it has been used to study the locomotion (i) in a complex fluid [27–34], (ii) in a gel [35,36], (iii) in a liquid crystal [37], (iv) in a porous media [38], (v) under confinement [2–4,39–45], (vi) at finite inertia of the fluid or the organism [2,46–48], and (vii) under transient effects [49]. The research on the locomotion under confinement has been restricted to the confinements caused by a rigid or soft wall [2,3,39–42,45], a plane clean interface [4], a deforming membrane [43], or a gel [44] with a Newtonian or a non-Newtonian suspending fluid.

Noting that any interface is inevitably covered with impurities that act as surfactants, it is essential to generalize the theory of locomotion near a clean interface to accommodate the effects of surfactant redistribution. Even though the locomotion under confinement depends on the swimmer's shape, most of the earlier research on the sheet's motion under confinement is devoted to a sheet passing transverse waves along its surface (or a Taylor swimming sheet [25]). To emphasize the influence of the swimmer's shape on locomotion and also to generalize the results associated with the sheet passing transverse waves, we analyze the motion of a sheet passing

*ardekani@purdue.edu

both longitudinal and transverse waves near a surfactant-laden interface.

This paper is organized as follows. We provide the governing equations and boundary conditions associated with the motion of a sheet near a plane surfactant-laden interface and present the perturbation technique and the solution methodology in Sec. II. We provide simple expressions for the swimming velocity under various limiting conditions in Sec. III. We then analyze the influence of surfactant redistribution on the swimming velocity of a sheet passing only transverse waves and that passing both longitudinal and transverse waves in Secs. IV A and IV B, respectively. We finally provide several concluding remarks in Sec. V and present the expressions for the flow field and the sheet’s velocity, and validate our results in the appendices.

II. MATHEMATICAL MODEL

Consider a 2D infinitely long sheet near a surfactant-laden interface (see Fig. 1 for schematic). We formulate this problem in a frame of reference moving with the swimming velocity of the sheet. The sheet deforms in such a manner that point $(x, 0)$ on its undeformed surface is located at (x_0, y_0) at time t , where x_0 and y_0 are given by

$$\begin{aligned} x_0 &= x + a \cos k(x + ct) + d \sin k(x + ct), \\ y_0 &= b \sin k(x + ct). \end{aligned} \tag{1}$$

Here a and d (b) are the amplitudes of longitudinal (transverse) waves while c and k are the wave speed and wave number, respectively.

For analytical tractability, we make the following assumptions. We assume the interface is plane and nondeforming;

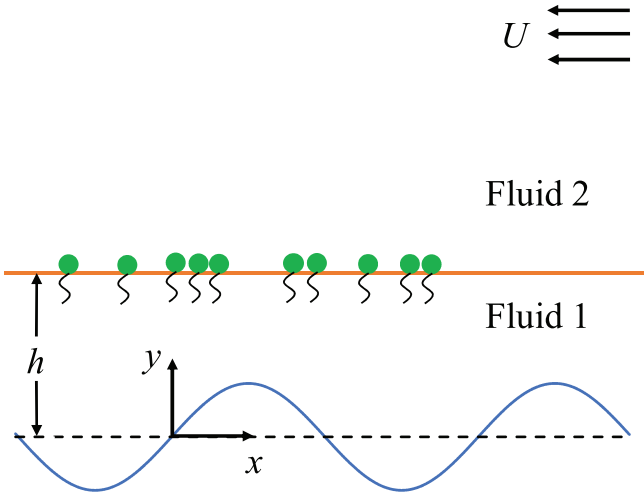


FIG. 1. A schematic showing a swimming sheet located near a plane surfactant-laden interface. The sheet propels by passing waves along its surface. The distance between the midplane of the sheet and the interface is h . We denote the fluid in which the swimmer is suspended as “Fluid 1” while the fluid above the interface is denoted as “Fluid 2.” In the frame moving with the swimming velocity of the sheet, a uniform streaming flow exists in fluid 2 far away from the sheet with the velocity that is negative of the sheet’s swimming velocity. The origin of the coordinate system is located at the midplane of the sheet.

such a nondeforming interface assumption is valid at small Capillary numbers (ratio of bulk viscous stresses to the capillary stresses). We assume the sheet is located symmetrically between two surfactant-laden interfaces which can occur for locomotion in a film [50–52]. Hence, we only solve for the fluid flow above the sheet. We assume the amplitude of the sheet’s deformation is much smaller than the wavelength, i.e., $ak \ll 1$, $bk \ll 1$, and $dk \ll 1$. Hence, we can write $ak = \epsilon \tilde{a}$, $bk = \epsilon \tilde{b}$, and $dk = \epsilon \tilde{d}$, where $\epsilon \ll 1$ while the magnitudes of \tilde{a} , \tilde{b} , and \tilde{d} can be at most $O(1)$. We denote the distance between the mid plane of the sheet and the interface by h , which is at least as large as the wavelength, i.e., $hk \geq O(1)$. The surfactant is insoluble and we neglect any kind of interfacial rheology imparted by the surfactant to the interface. Insoluble surfactant limit is valid when the interfacial transport of the surfactant is much faster than the bulk transport and the adsorption-desorption between the bulk fluid and the interface. Hence in this limit, the bulk surfactant does not influence the interfacial surfactant transport. Also, assuming the local surfactant concentration on the interface (Γ) is much smaller than the maximum possible surfactant concentration on the interface (Γ_∞), we use a linear constitutive equation to relate the interfacial tension (γ) to the surfactant concentration [53], i.e., $\gamma = \gamma_s - \Gamma RT$. Here γ_s is the interfacial tension of the clean interface, R is the ideal gas constant, and T is the absolute temperature.

We use the following characteristic parameters to scale all variables to dimensionless variables: a reference length $l_{\text{ref}} = 1/k$, reference velocity $u_{\text{ref}} = c$, reference time $t_{\text{ref}} = 1/(ck)$, reference pressure ($p_{\text{ref}}^{(j)}$), and stress ($T_{\text{ref}}^{(j)}$) in the j th fluid $p_{\text{ref}}^{(j)} = T_{\text{ref}}^{(j)} = \mu_j ck$, where μ_j is the dynamic viscosity of the j th fluid. As the problem is two dimensional, we use the stream function (ψ) to solve it. We nondimensionalize the stream function and surfactant concentration via $\psi_{\text{ref}} = c/k$ and $\Gamma_{\text{ref}} = \Gamma_{\text{eq}}$, respectively, where Γ_{eq} is the equilibrium surfactant concentration. We hereby formulate the problem of a sheet near a surfactant-laden interface in dimensionless variables.

As the inertia of the flow due to the swimming microorganism is typically negligible, the flow field is governed by the Stokes equations and the incompressibility condition. Using the relation between velocity components and the stream function, Eq. (2), the governing equations are simply the biharmonic equations for the stream functions, Eq. (3),

$$u^{(j)} = \frac{\partial \psi^{(j)}}{\partial y}; \quad v^{(j)} = -\frac{\partial \psi^{(j)}}{\partial x}, \quad \text{where } j = 1, 2, \tag{2}$$

$$\nabla^4 \psi^{(j)} = 0, \tag{3}$$

where $u^{(j)}$ and $v^{(j)}$ indicate the x and y components of the velocity of the j th fluid while $\psi^{(j)}$ denotes the stream function concerning the j th fluid. Point $(x, 0)$ on the undeformed sheet is located at (x_0, y_0) on the sheet’s surface at time t , where (x_0, y_0) is given by

$$\begin{aligned} x_0 &= x + \epsilon [\tilde{a} \cos(x + t) + \tilde{d} \sin(x + t)], \\ y_0 &= \epsilon \tilde{b} \sin(x + t). \end{aligned} \tag{4}$$

As the flow field in phase 1 should satisfy the no-slip and no-penetration boundary conditions on the sheet, we have

$$\begin{aligned} \left. \frac{\partial \psi^{(1)}}{\partial y} \right|_{(x_0, y_0)} &= \frac{\partial x_0}{\partial t} = \epsilon [-\tilde{a} \sin(x+t) + \tilde{d} \cos(x+t)], \\ \left. \frac{\partial \psi^{(1)}}{\partial x} \right|_{(x_0, y_0)} &= -\frac{\partial y_0}{\partial t} = -\epsilon \tilde{b} \cos(x+t). \end{aligned} \quad (5)$$

Either neglecting gravity or by assuming the density of the sheet is the same as the density of the fluid in which it is suspended, we find that the external force on the sheet is zero. Consequently, due to negligible inertia of the sheet, the net hydrodynamic force on the sheet must be zero, i.e., $\int_{\text{Sheet}} \mathbf{n} \cdot \mathbf{T}^{(1)}|_{\text{Sheet}} dS = \mathbf{0}$, which simplifies to

$$\int_0^{2\pi} \{-\epsilon \tilde{b} \cos(x+t) \mathbf{i} + [1 - \epsilon \tilde{a} \sin(x+t) + \epsilon \tilde{d} \cos(x+t)] \mathbf{j}\} \cdot \mathbf{T}^{(1)}|_{(x_0, y_0)} dx = \mathbf{0}, \quad (6)$$

where \mathbf{i} and \mathbf{j} denote the unit vectors along x and y directions, respectively. Also, \mathbf{n} is the normal to the sheet pointing into fluid 1 while $\mathbf{T}^{(j)}$ is the stress tensor for the j th fluid. Using the Newtonian fluid constitutive equation, $\mathbf{T}^{(j)}$ can be written in terms of pressure ($p^{(j)}$) and velocity fields ($\mathbf{v}^{(j)}$) of the j th fluid as $\mathbf{T}^{(j)} = -p^{(j)} \mathbf{I} + [\nabla \mathbf{v}^{(j)} + (\nabla \mathbf{v}^{(j)})^\dagger]$, where \dagger stands for the transpose and \mathbf{I} is an identity tensor. Far away from the sheet, the velocity of fluid 2 should approach the negative of the sheet's swimming velocity ($\mathbf{U} = U\mathbf{i}$). In terms of stream function, this condition simplifies to

$$\text{as } y \rightarrow \infty, \quad \psi^{(2)} \sim -Uy. \quad (7)$$

Since the interface is nondeforming, the fluid velocity (in both phases) at the interface but normal to the interface must be zero,

$$\text{at } y = h: \quad \frac{\partial \psi^{(1)}}{\partial x} = 0; \quad \frac{\partial \psi^{(2)}}{\partial x} = 0. \quad (8)$$

The fluid velocity at the interface but tangential to the interface must be continuous across the interface:

$$\text{at } y = h: \quad \frac{\partial \psi^{(1)}}{\partial y} = \frac{\partial \psi^{(2)}}{\partial y}. \quad (9)$$

Also, the jump in the tangential stresses across the interface should be balanced by the Marangoni stresses, which using the relationship between interfacial tension and the surfactant concentration simplifies to

$$\text{at } y = h: \quad \lambda T_{yx}^{(2)} - T_{yx}^{(1)} = \text{Ma} \frac{\partial \Gamma}{\partial x}; \quad \text{Ma} = \frac{RT\Gamma_{\text{eq}}}{\mu_1 c}, \quad (10)$$

where $T_{yx}^{(j)}$ denotes the yx component of the stress tensor in the j th fluid and the viscosity ratio $\lambda = \mu_2/\mu_1$. Finally, the transport of an insoluble surfactant on a nondeforming interface is governed by

$$\text{Pe}_s \left[\frac{\partial \Gamma}{\partial t} + \frac{\partial}{\partial x} (\Gamma u|_{y=h}) \right] = \frac{\partial^2 \Gamma}{\partial x^2}; \quad \text{Pe}_s = \frac{c}{kD_s}, \quad (11)$$

where D_s is the surface or interface diffusivity of the surfactant and the slip of an interface is written as $u|_{y=h} = \frac{\partial \psi^{(1)}}{\partial y}|_{y=h} = \frac{\partial \psi^{(2)}}{\partial y}|_{y=h}$.

We compare our formulation with those of Taylor [25] and Katz [3], where Taylor considered a sheet in an unbounded fluid while Katz analyzed the motion of sheet located asymmetrically between two walls. In these two works, the inertia of the flow was negligible due to which the stream function was governed by the biharmonic equation. The shape of sheet in Katz's work is same as that considered by us but Taylor's sheet passes only transverse waves along positive x -direction [$x_0 = x$, $y_0 = \epsilon \tilde{b} \sin(x-t)$]. Katz worked in a frame moving with velocity $(U-1)\mathbf{i}$ unlike the frame moving with the velocity $U\mathbf{i}$ considered by us and Taylor. Due to the different sheet's shape (respectively, frame of reference) considered by Taylor (respectively, by Katz), the boundary condition on the sheet given in these two works is different from that reported here [Eq. (5)]. The force-free condition is identically satisfied for the Taylor's sheet in an unbounded fluid. As Katz considered a sheet asymmetrically located between two walls, the sum of hydrodynamic forces acting on the top and bottom surfaces of the sheet must be zero and this force-free condition of Katz reduces to Eq. (6) for a sheet symmetrically located between two walls. A far-field condition similar to Eq. (7) exists for a fluid in which the sheet is immersed in Taylor's work, but no such condition exists for a sheet bounded by walls as considered by Katz. To ensure the fluid does not penetrate the walls, Katz applied a condition similar to Eq. (8) at the walls. Instead of the continuous tangential velocity condition [Eq. (9)], shear stress balance condition [Eq. (10)], and the surfactant transport equation [Eq. (11)] at the interface, there is a no-slip boundary condition at the wall in Katz's work.

We need to solve Eqs. (3)–(11) to determine the swimming velocity of the sheet, $U\mathbf{i}$. As the surfactant transport equation is nonlinear, it is not possible to solve these equations analytically for an arbitrary value of ϵ . However, for $\epsilon \ll 1$, we can use the following traditional technique to find the leading order approximation of the sheet's swimming velocity: (i) express the boundary condition on the sheet's surface as a series of boundary conditions applied at the mid plane of the sheet by doing a Taylor series expansion of any function $f(x_0, y_0)$ about $(x, 0)$ and (ii) expand all the variables as a power series in ϵ :

$$\begin{aligned} &\{\mathbf{v}^{(j)}, \mathbf{T}^{(j)}, p^{(j)}, U, \psi^{(j)}, u|_{y=h}\} \\ &= \sum_{n=1}^{\infty} \epsilon^n \{\mathbf{v}_n^{(j)}, \mathbf{T}_n^{(j)}, p_n^{(j)}, U_n, \psi_n^{(j)}, u_n|_{y=h}\}, \\ &\Gamma = 1 + \sum_{n=1}^{\infty} \epsilon^n \Gamma_n. \end{aligned} \quad (12)$$

The resulting perturbed equations are linear and have the following general solution for the stream function and the surfactant concentration at $O(\epsilon^n)$:

$$\begin{aligned} \psi_n^{(1)} &= \sum_{m=1}^{\infty} \{[(A_{n,m}^{(1)} + E_{n,m}^{(1)}y) \cos m(x+t) \\ &+ (B_{n,m}^{(1)} + F_{n,m}^{(1)}y) \sin m(x+t)] \cosh my \\ &+ [(C_{n,m}^{(1)} + G_{n,m}^{(1)}y) \cos m(x+t) \\ &+ (D_{n,m}^{(1)} + H_{n,m}^{(1)}y) \sin m(x+t)] \sinh my\} \\ &+ \alpha_n y + \beta_n y^2 + \gamma_n y^3, \end{aligned} \quad (13)$$

$$\begin{aligned} \psi_n^{(2)} = & -U_n y + \sum_{m=1}^{\infty} [(A_{n,m}^{(2)} + E_{n,m}^{(2)}) \cos m(x+t) \\ & + (B_{n,m}^{(2)} + F_{n,m}^{(2)}) \sin m(x+t)] e^{-my}, \end{aligned} \quad (14)$$

$$\Gamma_n = \sum_{m=1}^{\infty} [J_{n,m} \cos m(x+t) + L_{n,m} \sin m(x+t)], \quad (15)$$

where $A_{n,m}^{(1)}$, $B_{n,m}^{(1)}$, $C_{n,m}^{(1)}$, $D_{n,m}^{(1)}$, $E_{n,m}^{(1)}$, $F_{n,m}^{(1)}$, $G_{n,m}^{(1)}$, $H_{n,m}^{(1)}$, $A_{n,m}^{(2)}$, $B_{n,m}^{(2)}$, $E_{n,m}^{(2)}$, $F_{n,m}^{(2)}$, α_n , β_n , γ_n , $J_{n,m}$, and $L_{n,m}$ are unknown constants that need to be determined while satisfying the perturbed boundary conditions. The expressions of the constants that determine the $O(\epsilon)$ and $O(\epsilon^2)$ flow fields along with the expression of the leading order swimming velocity U_2 are provided in Appendix A. We also verify our calculation by comparing the leading order swimming velocity of the sheet U_2 with that reported in the literature in various limits. This validation is presented in Appendix B.

III. LIMITING CASES

We note that the swimming velocity depends in a complex fashion on Ma and Pe_s as can be seen in Eq. (A15) derived for a sheet passing transverse waves near an air-water interface. So, to understand the surfactants influence on the swimming velocity U , we need to numerically evaluate U for various Ma and Pe_s . Before doing this, in this section we report some simple expressions for the swimming velocity in the limits of small or large Ma or Pe_s . Through such expressions, one can easily find out how the surfactant redistribution affects the swimming velocity. We report these limiting forms for a sheet near an air-water interface ($\lambda = 0$) by noting that the leading order swimming occurs at $O(\epsilon^2)$, i.e., $U = \epsilon^2 U_2 + O(\epsilon^4)$.

At small Ma , we get

$$\begin{aligned} U_2 = & U_{2,\text{clean}} + \frac{\text{Pe}_s \text{Ma}}{(\text{Pe}_s^2 + 1)[\sinh(2h) - 2h]^2} \\ & \times [(h^2 \cosh(2h) - 2h \sinh(2h) + h^2 + \cosh(2h) - 1) \\ & \times \tilde{b}(\tilde{a} - \text{Pe}_s \tilde{d}) + [h \sinh(2h) - \cosh(2h) + 1] \tilde{b}^2 h] \\ & + O(\text{Ma}^2). \end{aligned} \quad (16)$$

Here $U_{2,\text{clean}}$ is the swimming velocity near a plane clean interface whose expression for $\tilde{a} = \tilde{d} = 0$ is given in Eq. (B3). We see that the correction due to surfactant redistribution depends nonlinearly on Pe_s . As long as $\tilde{d} = 0$, we see that the surfactant redistribution increases the sheet's velocity because $[h \sinh(2h) - \cosh(2h) + 1] > 0$ and $[h^2 \cosh(2h) - 2h \sinh(2h) + h^2 + \cosh(2h) - 1] > 0$ for all h . When $\tilde{a} = 0$, the surfactant redistribution can increase or even decrease the sheet's velocity depending on whether the following ratio is respectively greater than or less than 1.

$$\frac{[h \sinh(2h) - \cosh(2h) + 1] h}{[h^2 \cosh(2h) - 2h \sinh(2h) + h^2 + \cosh(2h) - 1] \text{Pe}_s} \frac{\tilde{b}}{\tilde{d}}. \quad (17)$$

In the more general case when $\tilde{a} \neq 0$, $\tilde{d} \neq 0$, and $\tilde{b} \neq 0$, the surfactant redistribution can increase or decrease the swim-

mer's velocity depending on Pe_s , h , and relative order of magnitude of the wave amplitudes.

At small Pe_s , we get

$$\begin{aligned} U_2 = & U_{2,\text{clean}} + \frac{\text{Pe}_s \text{Ma} \times \tilde{b}}{[\sinh(2h) - 2h]^2} [\tilde{a}[h^2 \cosh(2h) \\ & - 2h \sinh(2h) + h^2 + \cosh(2h) - 1] \\ & + \tilde{b} h [h \sinh(2h) - \cosh(2h) + 1]] + O(\text{Pe}_s^2). \end{aligned} \quad (18)$$

From this expression, we see that the swimming velocity does not depend on “ d ” modes. Also as $[h^2 \cosh(2h) - 2h \sinh(2h) + h^2 + \cosh(2h) - 1] > 0$ and $[h \sinh(2h) - \cosh(2h) + 1] > 0$, we see that the surfactant redistribution always increases the swimming velocity at small Pe_s . This is in contrast with the observation that the surfactant redistribution can increase or even decrease the velocity of a swimming microorganism inside a surfactant-laden drop at small Pe_s [20]. These different influences of the surfactant on the swimming velocity, reported in Ref. [20] and this work, is due to different shapes of the swimmer and the interface used in these two works.

At large Ma , we get

$$\begin{aligned} U_2 = & U_{2,\text{wall}} - \frac{4\tilde{b}}{\text{Pe}_s \text{Ma} [2h^2 - \cosh(2h) + 1]^2} \\ & \times [(h^2 \cosh(2h) - 2h \sinh(2h) + h^2 + \cosh(2h) - 1) \\ & \times (\tilde{a} + \tilde{d} \times \text{Pe}_s) + [h \sinh(2h) \\ & - \cosh(2h) + 1] \tilde{b} h] + O(\text{Ma}^{-2}). \end{aligned} \quad (19)$$

Here $U_{2,\text{wall}}$ is the swimming velocity near a plane wall whose expression is given in Eq. (B2). Again as $[h^2 \cosh(2h) - 2h \sinh(2h) + h^2 + \cosh(2h) - 1] > 0$ and $[h \sinh(2h) - \cosh(2h) + 1] > 0$, we see that the swimming velocity near a surfactant-laden interface at large Ma is always less than that near a plane wall.

IV. RESULTS

In this section, we examine the influence of surfactant redistribution on the swimming velocity of the sheet near a surfactant-laden interface.

It was reported that the swimming velocity of a sheet, propagating longitudinal waves, near a plane wall is the same as its velocity in an unbounded fluid [3], i.e., $U = -\frac{\epsilon^2}{2}(\tilde{a}^2 + \tilde{d}^2) + O(\epsilon^4)$. Our analysis suggests the presence of a surfactant-laden interface instead of a wall near such a sheet, does not modify its velocity, i.e., the velocity of a sheet propagating longitudinal waves near a plane surfactant-laden interface is the same as its velocity in an unbounded fluid.

As we have analyzed the velocity of a sheet propagating longitudinal waves near a plane surfactant-laden interface, we then proceed to examine the velocity of a sheet (near a surfactant-laden interface) passing only transverse waves and that passing both longitudinal and transverse waves in the following two subsections. Even though the expressions for the leading order swimming velocity are derived for any arbitrary viscosity ratio λ , we only report the influence of surfactant redistribution on this velocity for an air-water

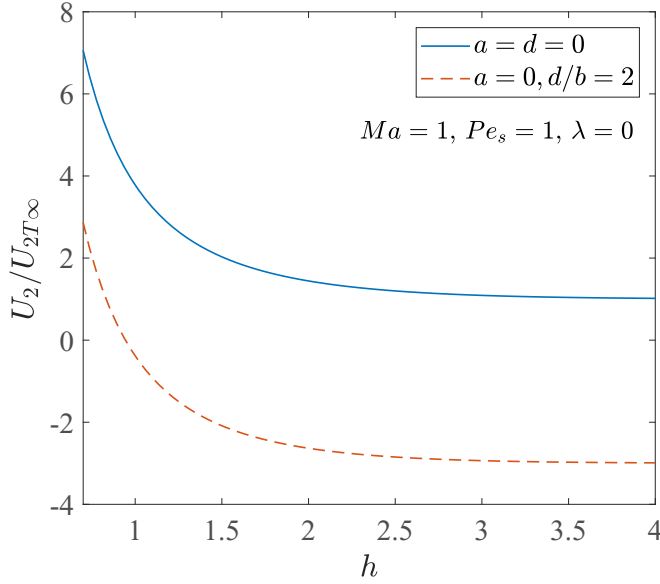
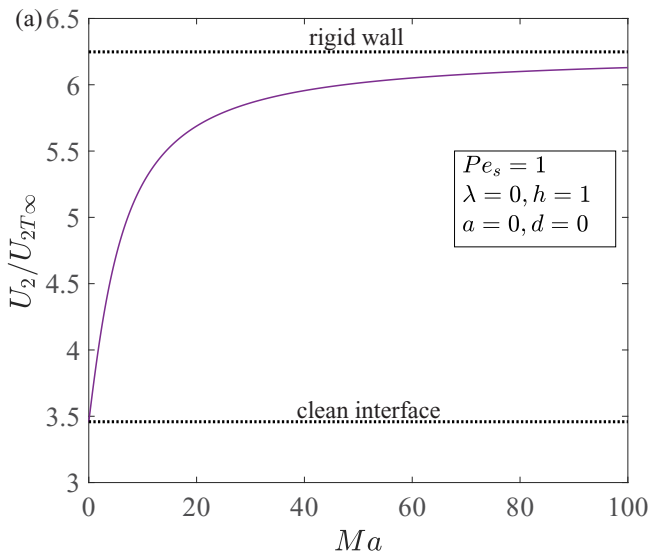


FIG. 2. The variation of the swimming velocity with the distance between the interface and (the mid plane of) the sheet for a sheet passing only transverse waves (blue solid line) and that passing both longitudinal and transverse waves (red dashed line). Here the swimming velocity is normalized with the swimming velocity of a sheet passing only transverse waves in an unbounded fluid ($U_{2T\infty}$). The viscosity ratio $\lambda = 0$, Marangoni number $Ma = 1$, and the surface Péclet number $Pe_s = 1$.

interface ($\lambda = 0$) as experiments on locomotion in films are mainly performed for an air-water interface [50–52].

For a fixed Ma and Pe_s , we found that the swimming velocity increases as h decreases (see Fig. 2). A similar trend with decreasing h was reported for confinements caused by a rigid plane wall [3], a plane clean interface [4], or a gel [44]. Also, the variation of the swimming velocity with Ma



and Pe_s is qualitatively the same for any fixed value of h . For this reason, we report and analyze this variation with Ma and Pe_s for a typical value of $h = 1$.

We report here the typical values of Ma and Pe_s . For the tail of a spermatozoan [54], the wave speed $c \sim (200\text{--}1200) \times 10^{-6}$ m/s and the wave number $k \sim (1.14\text{--}4.18) \times 10^5$ m $^{-1}$. The maximum possible surfactant concentration at an air-water interface [55,56] $\Gamma_\infty \sim 10^{-6}\text{--}10^{-4}$ mol/m 2 . Assuming that the equilibrium surfactant concentration $\Gamma_{\text{eq}} \sim (10^{-3}\text{--}10^{-1})\Gamma_\infty$, we get $\Gamma_{\text{eq}} \sim (10^{-9}\text{--}10^{-5})$ mol/m 2 . The surface diffusivity of the surfactant [57] $D_s \sim (1\text{--}10) \times 10^{-9}$ m 2 /s. Using the definitions of Ma , Pe_s , along with the viscosity of water (μ_1) and the temperature of $T = 298$ K, we get $Ma \sim O(1)\text{--}O(10^5)$ and $Pe_s \sim 0.05\text{--}O(10)$.

A. Sheet passing only transverse wave along its surface

When a sheet passing only transverse waves is located near a plane surfactant-laden interface, the dependence of its swimming velocity on Ma (for a fixed Pe_s) and on Pe_s (for a fixed Ma) is given in Fig. 3. We observe the following from this figure. As the minimum velocity occurs at $Ma = 0$ or $Pe_s \rightarrow 0$ and since $Ma = 0$ or $Pe_s \rightarrow 0$ represents a clean interface, we conclude that the swimming velocity near a plane surfactant-laden interface is always more than that near a plane clean interface. Near a plane surfactant-laden interface, (a) the swimming velocity increases with an increase in Ma for any fixed Pe_s , (b) it increases with an increase in Pe_s for any fixed but large Ma , i.e., $Ma \geq O(10)$, and (c) it initially increases and then decreases with an increase in Pe_s for any fixed but small Ma , i.e., $Ma \leq O(1)$.

B. Sheet passing both longitudinal and transverse waves along its surface

In this section, we discuss how the effect of surfactant redistribution on the swimming velocity gets modified, in

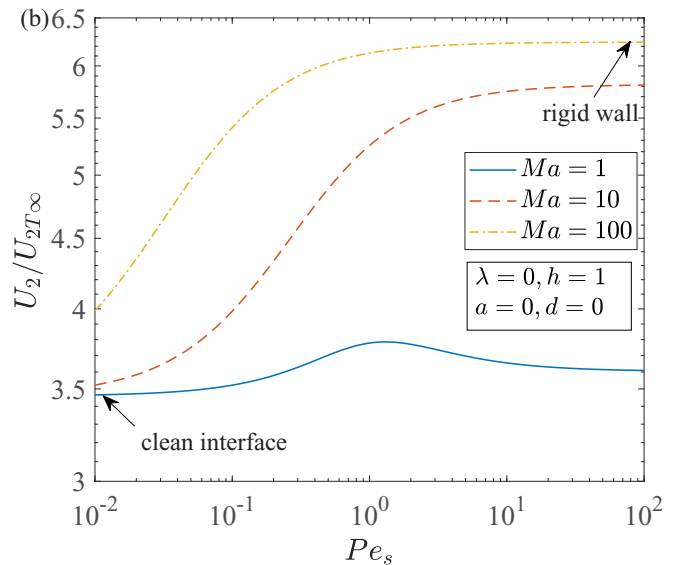


FIG. 3. For a sheet passing transverse waves near a plane surfactant-laden interface, the variation of the leading order swimming velocity with (a) Ma for $Pe_s = 1$ and (b) Pe_s for $Ma = 1, 10$, and 100 . Here the swimming velocity is normalized with the swimming velocity of the same sheet in an unbounded fluid ($U_{2T\infty}$). The distance between the midplane of the sheet and the interface is $h = 1$, the viscosity ratio $\lambda = 0$, and the amplitudes of the longitudinal waves $a = d = 0$.

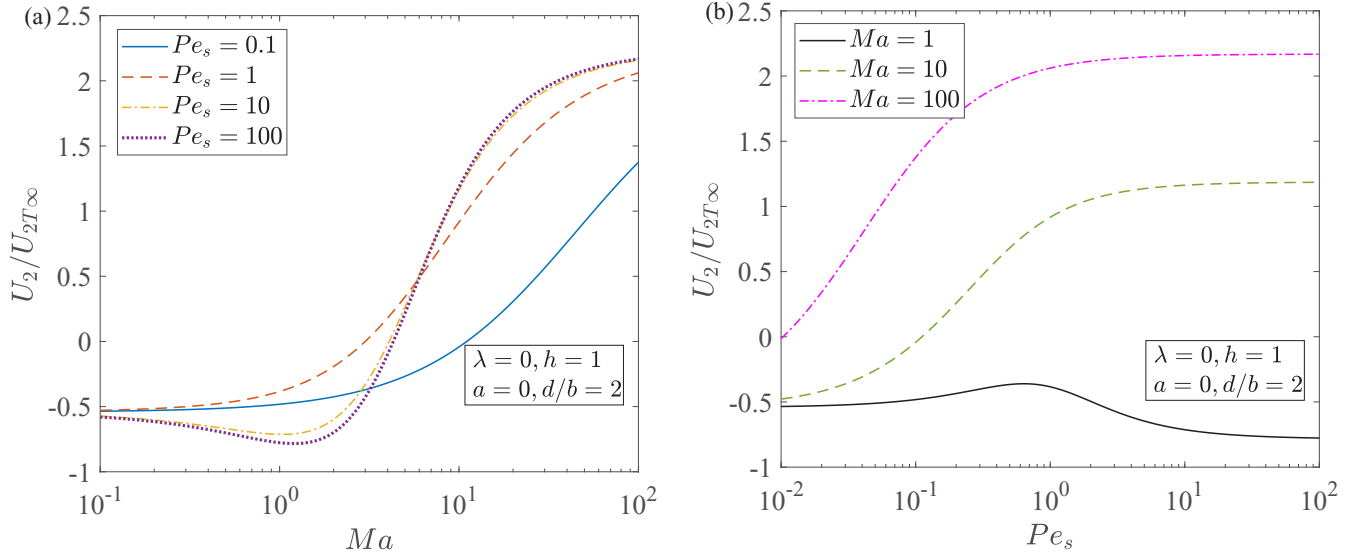


FIG. 4. For a sheet passing both longitudinal and transverse waves near a plane surfactant-laden interface, the variation of the leading order swimming velocity with (a) Ma for $Pe_s = 0.1, 1, 10, 100$ and with (b) Pe_s for $Ma = 1, 10, 100$. Here the swimming velocity is normalized with the swimming velocity of a sheet passing transverse waves in an unbounded fluid ($U_{2T\infty}$). The distance between the midplane of the sheet and the interface is $h = 1$, the viscosity ratio $\lambda = 0$, and the amplitudes of the waves $a = 0$, and $d/b = 2$.

comparison to this effect presented in the earlier section, if a sheet is passing both longitudinal and transverse waves along its surface. For this purpose, we plot the variation of the swimming velocity with Ma (for a fixed Pe_s) and Pe_s (for a fixed Ma) in Fig. 4. From this figure, we observe the following. The swimming velocity for a sheet near a plane surfactant-laden interface can be more or even less than that for a sheet near a plane clean interface ($Ma \rightarrow 0$ or $Pe_s \rightarrow 0$). Unlike the case of a sheet passing only transverse waves, the swimming velocity near a surfactant-laden interface might not lie in between the swimming velocity near a plane clean interface and that near a plane wall. Desai *et al.* [11] reported a similar observation by noting that the critical trapping radius of a surfactant-laden drop is less than those of a clean drop and a rigid sphere where a particle or a drop would trap a nearby swimming microorganism if their radius is more than the critical trapping radius. When a sheet is in the vicinity of a surfactant-laden interface, (a) the swimming velocity increases with an increase in Ma for a fixed but small Pe_s [$\ll O(1)$], (b) it initially decreases and then increases with an increase in Ma for a fixed but large Pe_s [$\geq O(10)$], (c) it increases with an increase in Pe_s for a fixed yet large Ma [$\geq O(10)$], and (d) it initially increases and then decreases with an increase in Pe_s for a fixed but small Ma [$\leq O(1)$].

It seems nonintuitive for the swimming velocity near a surfactant-laden interface to lie outside the range corresponding to the one near a clean interface and a rigid wall. If we had a rigid particle moving near a surfactant-laden interface due to some fixed force acting on it, its velocity always lies in between its velocities near a clean interface and a plane wall [58]. So, the motion of organisms is defying the intuition built on the basis of particle motion. This is not the first time that such phenomenon is reported. Considering the motion of particles or organisms in complex fluids, we find that the particle experiencing a fixed force moves faster in a shear-thinning fluid than that in a Newtonian fluid but the velocity

of a swimming microorganism in a shear-thinning fluid can be more or even less than that in a Newtonian fluid [59]. A similar observation has been made for the velocity of a swimming microorganism in a viscoelastic fluid [33].

Even though most of the observations in Figs. 3 and 4 can be qualitatively explained by analyzing the influence of surfactant redistribution on the amplitude of leading order interface slip (see Appendix C), such reasoning is not useful to understand the swimming velocity near a surfactant-laden interface if this velocity lies outside the range bounded by

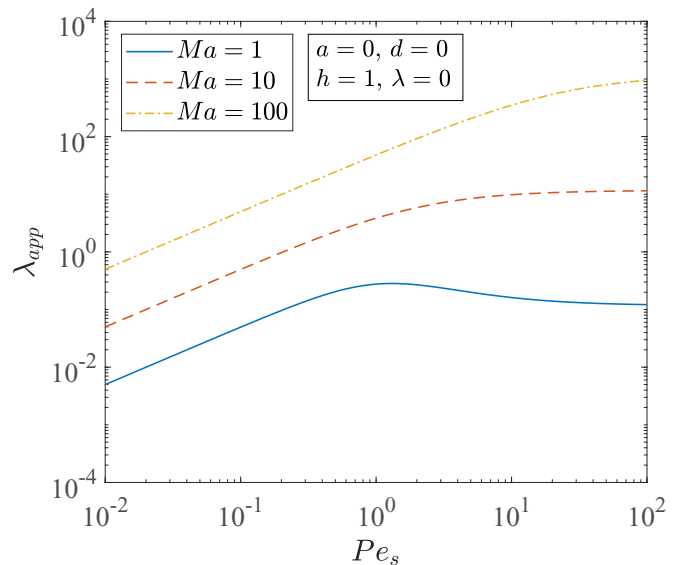


FIG. 5. The variation of apparent viscosity ratio with Pe_s at $Ma = 1$ (blue solid line), 10 (red dashed line), and 100 (yellow dash-dotted line). Here, the sheet is passing only transverse waves, hence $a = d = 0$. The actual viscosity ratio of the surfactant-laden interface $\lambda = 0$ while $h = 1$.

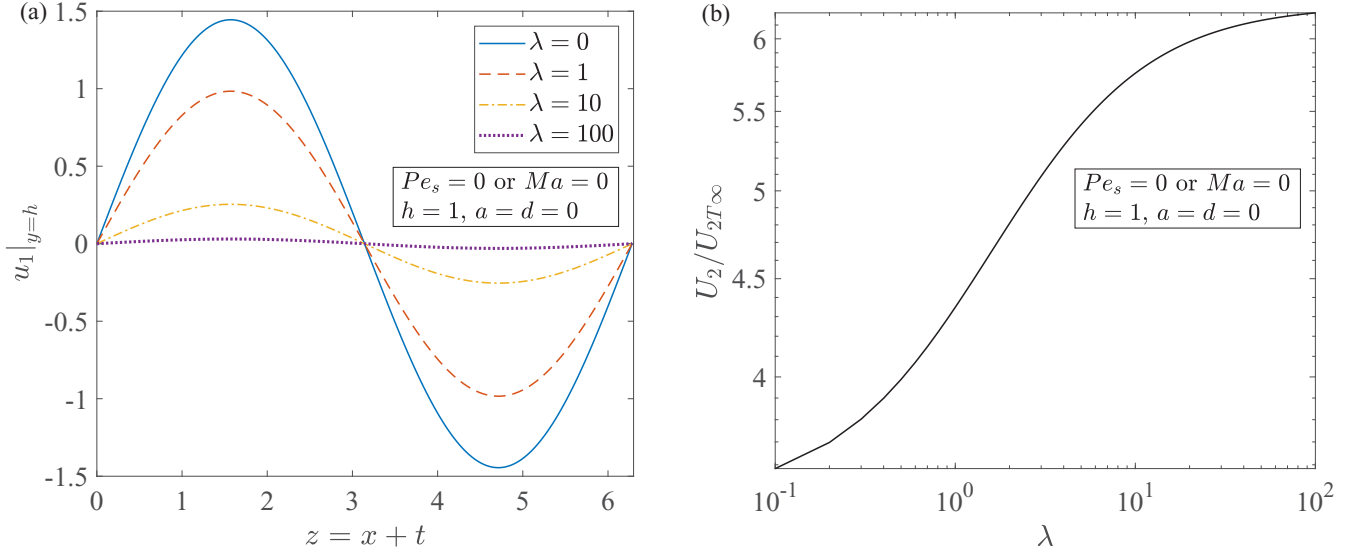


FIG. 6. For a sheet passing transverse waves near a plane clean interface, the variation of the (a) leading order interface slip and (b) leading order swimming velocity with the viscosity ratio λ . Here the swimming velocity is normalized with the swimming velocity of the same sheet in an unbounded fluid ($U_{2T\infty}$). The values of the other parameters h , a , and d are kept the same as those of Fig. 3.

the velocities near a clean interface and a plane wall. Consequently, the amplitude of leading order interface slip is not determinative of the swimming velocity changes. Hence to get a proper understanding of the variation of the swimming velocity with all values of Ma and Pe_s , we need to correlate the surfactant induced changes in either (i) the amplitude and phase of the leading order slip (not just the amplitude) or (ii) the second-order slip (instead of first-order slip) with the swimming velocity which are not done in this work.

C. Apparent viscosity ratio

As the expression for the swimming velocity of a sheet near a surfactant-laden interface is quite lengthy, we represent the

surfactant-laden interface as a clean interface with a modified or apparent viscosity ratio (λ_{app}) to convey the effects of surfactant redistribution in a succinct manner. The expression for λ_{app} is simpler than the expression for the swimming velocity. Using this expression for λ_{app} and the dependence of the sheet's velocity on the viscosity ratio for a sheet near a clean interface [4], we can evaluate the sheet's velocity at this apparent viscosity ratio to find its velocity near a surfactant-laden interface. To determine the apparent viscosity ratio, we simply equate the sheet's velocity near a surfactant-laden interface with zero viscosity ratio to its velocity near a clean interface with a viscosity ratio that is equal to the apparent viscosity ratio. We then solve this equation for the apparent viscosity ratio to obtain

$$\lambda_{app} = \frac{\text{Ma Pe}_s \left(\begin{aligned} & [(-\text{Ma Pe}_s \tilde{a} - 2\tilde{b})h - 2\tilde{d} \text{Pe}_s + 2\tilde{a}][\cosh(h)]^3 \\ & - 2 \{[(1/2 \text{Ma } \tilde{b} - \tilde{d})\text{Pe}_s + \tilde{a}]h - 1/2 \text{Ma Pe}_s \tilde{a}\} \sinh(h)[\cosh(h)]^2 \\ & + \left(\text{Ma Pe}_s \tilde{a} h^3 + (-2\tilde{d} \text{Pe}_s + 2\tilde{a})h^2 \right. \\ & \quad \left. + (\text{Ma Pe}_s \tilde{a} + 2\tilde{b})h + 2\tilde{d} \text{Pe}_s - 2\tilde{a} \right) \cosh(h) \\ & - \left(-\text{Ma Pe}_s \tilde{b} h^3 + (\text{Ma Pe}_s \tilde{a} - 2\tilde{b})h^2 \right. \\ & \quad \left. + [(-\text{Ma } \tilde{b} - 2\tilde{d})\text{Pe}_s + 2\tilde{a}]h + \text{Ma Pe}_s \tilde{a} \right) \sinh(h) \end{aligned} \right)}{\left[\begin{aligned} & \{[-2 \text{Ma } \tilde{d} - 4\tilde{b})\text{Pe}_s^2 - 2 \text{Ma Pe}_s \tilde{a} - 4\tilde{b})h + 4 \text{Pe}_s^2 \tilde{a} + 4\tilde{a}\}[\cosh(h)]^3 \\ & - 4 \{(\text{Pe}_s^2 \tilde{a} + 1/2 \tilde{b} \text{Ma Pe}_s + \tilde{a})h - 1/2 \text{Ma Pe}_s (\tilde{d} \text{Pe}_s + \tilde{a})\} \sinh(h)[\cosh(h)]^2 \\ & + \left(2 \text{Ma Pe}_s (\tilde{d} \text{Pe}_s + \tilde{a})h^3 + (4 \text{Pe}_s^2 \tilde{a} + 4\tilde{a})h^2 \right. \\ & \quad \left. + [(2 \text{Ma } \tilde{d} + 4\tilde{b})\text{Pe}_s^2 + 2 \text{Ma Pe}_s \tilde{a} + 4\tilde{b})h - 4 \text{Pe}_s^2 \tilde{a} - 4\tilde{a} \right) \cosh(h) \\ & - 2 \left(-\text{Ma Pe}_s \tilde{b} h^3 + [(\text{Ma } \tilde{d} - 2\tilde{b})\text{Pe}_s^2 + \text{Ma Pe}_s \tilde{a} - 2\tilde{b})h^2 \right. \\ & \quad \left. + (-\tilde{b} \text{Ma Pe}_s + 2 \text{Pe}_s^2 \tilde{a} + 2\tilde{a})h + \text{Ma Pe}_s (\tilde{d} \text{Pe}_s + \tilde{a}) \right) \sinh(h) \end{aligned} \right]}, \quad (20)$$

which simplifies for a sheet passing only transverse waves to

$$\lim_{\tilde{a} \rightarrow 0, \tilde{d} \rightarrow 0} \lambda_{app} = \frac{2 \text{Ma Pe}_s [-\sinh(2h) - 1/2 \text{Ma Pe}_s \cosh(2h) + \text{Ma}(h^2 + 1/2)\text{Pe}_s + 2h]}{(-4 \text{Pe}_s^2 - 4) \sinh(2h) - 2 \text{Ma Pe}_s \cosh(2h) + 8 \text{Pe}_s^2 h + (4h^2 + 2)\text{Ma Pe}_s + 8h}. \quad (21)$$

In the limit $Ma \rightarrow 0$ or $Pe_s \rightarrow 0$, the surfactant-laden interface behaves like a clean interface due to which λ_{app} approaches the actual viscosity ratio that is zero. Hence, $\lambda_{app} \rightarrow 0$ as $Ma \rightarrow 0$ or $Pe_s \rightarrow 0$. In the limit $Ma \rightarrow \infty$, the surfactant becomes incompressible [10,58] and the surfactant-laden interface behaves like a rigid wall (see Appendix B for discussion on the incompressible surfactant). Hence, $\lambda_{app} \rightarrow \infty$ as $Ma \rightarrow \infty$. As $Pe_s \rightarrow \infty$, λ_{app} approaches a constant value given by

$$\lim_{Pe_s \rightarrow \infty, \tilde{a} \rightarrow 0, \tilde{d} \rightarrow 0} \lambda_{app} = \frac{Ma^2 \{[\cosh(h)]^2 - h^2 - 1\}}{4 \sinh(h) \cosh(h) - 4h}, \quad (22)$$

for a sheet passing only transverse waves.

For a sheet passing transverse waves near a surfactant-laden interface, typical variation of λ_{app} with Pe_s for various Ma is shown in Fig. 5. From this figure, we observe that λ_{app} increases with an increase in Pe_s at large Ma [$\geq O(10)$] while it initially increases and then decreases with an increase in Pe_s at small Ma [$\leq O(1)$]. Combining this dependence of λ_{app} on Ma , Pe_s with the dependence of U_2 on λ for a sheet near a clean interface [Fig. 6(b)], we expect the velocity of a sheet near a surfactant-laden interface to increase monotonically (respectively, vary nonmonotonically) with an increase in Pe_s at large Ma (respectively, at small Ma), consistent with the observations of Fig. 3(b).

V. CONCLUSIONS

We aimed to understand the dependence of a microorganism's swimming velocity on the Marangoni number (Ma) and the surface Péclet number (Pe_s) when it is near a surfactant covered interface. For this purpose, we derived the velocity of a 2D infinitely long swimming sheet near a surfactant-laden interface under the assumptions of zero Reynolds number,

zero interface deformation, and small sheet's deformation. We observed that the swimming velocity near a surfactant-laden interface can be more or even less than that near a clean interface and this velocity varies nonmonotonically with Ma and Pe_s , these observations being highly sensitive to the type of wave passing through the sheet. Unlike the rigid particles near a surfactant-laden interface, we found that the swimming microorganisms near such an interface can have a velocity that does not lie in between their velocities near a clean interface and a rigid wall. To succinctly express the effects of surfactant redistribution, we represented the surfactant-laden interface as a clean interface with a viscosity ratio equal to an apparent viscosity ratio whose expression is found by equating the swimming velocities near a clean and surfactant-laden interface.

ACKNOWLEDGMENT

This research was supported by National Science Foundation Grants No. CBET-1700961 and No. CBET-1604423.

APPENDIX A: EXPRESSIONS FOR CONSTANTS THAT APPEAR IN STREAM FUNCTION AND SURFACTANT CONCENTRATION

In this section, we provide expressions for the constants appearing in Eqs. (13)–(15) that enable us to determine the stream function and the surfactant concentration at various orders of ϵ . Even though we derived these expressions for any arbitrary viscosity ratio λ and for nonzero wave amplitudes $\tilde{a} \neq 0$, $\tilde{b} \neq 0$, and $\tilde{d} \neq 0$, as these expressions are lengthy, we provide these expressions only for the special case of an air-water interface ($\lambda = 0$) and a sheet passing only transverse waves ($\tilde{a} = 0$, $\tilde{d} = 0$).

1. Expressions for constants appearing in $O(\epsilon)$ stream function and surfactant concentration

Here, we present the expressions for constants appearing in $\psi_1^{(1)}$, $\psi_1^{(2)}$, and Γ_1 .

$$A_{1,1}^{(1)} = 0, \quad (A1)$$

$$B_{1,1}^{(1)} = -\tilde{b}, \quad (A2)$$

$$-C_{1,1}^{(1)} = E_{1,1}^{(1)} = \frac{2[\sinh(h)]^2 Pe_s^2 Ma \tilde{b} h^2}{\mathcal{D}}, \quad (A3)$$

$$-D_{1,1}^{(1)} = F_{1,1}^{(1)} = \frac{\left(\begin{aligned} &-4Ma[\cosh(h)]^4 Pe_s - [(Ma^2 + 4)Pe_s^2 + 4] \sinh(h)[\cosh(h)]^3 \\ &+ [(-Ma^2 h + 4h)Pe_s^2 + (2h^2 + 4)MaPe_s + 4h][\cosh(h)]^2 \\ &+ Ma^2 Pe_s^2 \sinh(h)(h^2 + 1) \cosh(h) + h Pe_s Ma [Ma(h^2 + 1)Pe_s + 2h] \end{aligned} \right) \tilde{b}}{\mathcal{D}}, \quad (A4)$$

$$G_{1,1}^{(1)} = \frac{-2 Pe_s^2 h Ma \tilde{b} \sinh(h)[\cosh(h)h - \sinh(h)]}{\mathcal{D}}, \quad (A5)$$

$$H_{1,1}^{(1)} = \frac{-\sinh(h)\tilde{b} \left(\begin{aligned} &-4 Ma Pe_s [\cosh(h)]^3 - [(Ma^2 + 4)Pe_s^2 + 4] \sinh(h)[\cosh(h)]^2 \\ &+ (4Pe_s^2 h + (2h^2 + 4)MaPe_s + 4h) \cosh(h) \\ &+ Pe_s \sinh(h) Ma [Ma(h^2 + 1)Pe_s + 2h] \end{aligned} \right)}{\mathcal{D}}, \quad (A6)$$

$$A_{1,1}^{(2)} = -\frac{2h^2 e^h Ma \sinh(h) Pe_s^2 \tilde{b} \{[\cosh(h)]^2 - h^2 - 1\}}{\mathcal{D}}, \quad (A7)$$

$$B_{1,1}^{(2)} = \frac{2h^2\tilde{b}(-\text{Ma}[\cosh(h)]^2\text{Pe}_s + (-2\text{Pe}_s^2 - 2)\sinh(h)\cosh(h) + 2\text{Pe}_s^2h + \text{Ma}(h^2 + 1)\text{Pe}_s + 2h)\sinh(h)e^h}{\mathcal{D}}, \quad (\text{A8})$$

$$E_{1,1}^{(2)} = \frac{2e^h\text{Ma}\sinh(h)\text{Pe}_s^2\tilde{b}h\{[\cosh(h)]^2 - h^2 - 1\}}{\mathcal{D}}, \quad (\text{A9})$$

$$F_{1,1}^{(2)} = \frac{-2h\tilde{b}(-\text{Ma}[\cosh(h)]^2\text{Pe}_s + (-2\text{Pe}_s^2 - 2)\sinh(h)\cosh(h) + 2\text{Pe}_s^2h + \text{Ma}(h^2 + 1)\text{Pe}_s + 2h)\sinh(h)e^h}{\mathcal{D}}, \quad (\text{A10})$$

$$J_{1,1} = \frac{2h\text{Pe}_s\sinh(h)\tilde{b}\{-\text{Ma}[\cosh(h)]^2\text{Pe}_s - 2\cosh(h)\sinh(h) + \text{Ma}(h^2 + 1)\text{Pe}_s + 2h\}}{\mathcal{D}}, \quad (\text{A11})$$

$$L_{1,1} = \frac{4\text{Pe}_s^2\tilde{b}h\sinh(h)[- \cosh(h)\sinh(h) + h]}{\mathcal{D}}, \quad (\text{A12})$$

where

$$\begin{aligned} \mathcal{D} = & [(\text{Ma}^2 + 4)\text{Pe}_s^2 + 4][\cosh(h)]^4 + 4\text{Ma}[\cosh(h)]^3\sinh(h)\text{Pe}_s + \{-4 + [-4 + (-2h^2 - 2)\text{Ma}^2] \\ & \times \text{Pe}_s^2 - 4\text{Ma}\text{Pe}_s h\}[\cosh(h)]^2 - 4[2\text{Pe}_s^2h + \text{Ma}(h^2 + 1)\text{Pe}_s + 2h]\sinh(h)\cosh(h) \\ & + [(h^2 + 1)^2\text{Ma}^2 + 4h^2]\text{Pe}_s^2 + 4h\text{Ma}(h^2 + 1)\text{Pe}_s + 4h^2, \\ U_1 = \alpha_1 = \beta_1 = \gamma_1 = & 0. \end{aligned} \quad (\text{A13})$$

2. Expressions for constants appearing in $O(\epsilon^2)$ stream function

Here, we present the expressions for constants appearing in $\psi_2^{(1)}$ and $\psi_2^{(2)}$.

$$\beta_2 = \gamma_2 = 0, \quad (\text{A14})$$

$$U_2 = -\alpha_2 = \frac{-\left(\begin{aligned} & [-4 + (-\text{Ma}^2 - 4)\text{Pe}_s^2][\cosh(h)]^4 - 4\sinh(h)[\cosh(h)]^3\text{Ma}\text{Pe}_s \\ & + [4 + (2\text{Ma}^2 + 4)\text{Pe}_s^2][\cosh(h)]^2 + 4\sinh(h)\cosh(h)\text{Ma}\text{Pe}_s \\ & + [(h^4 - 1)\text{Ma}^2 + 4h^2]\text{Pe}_s^2 + 4\text{Ma}\text{Pe}_s h^3 + 4h^2 \end{aligned} \right) \tilde{b}^2}{\left[\begin{aligned} & [(2\text{Ma}^2 + 8)\text{Pe}_s^2 + 8][\cosh(h)]^4 + 8\sinh(h)[\cosh(h)]^3\text{Ma}\text{Pe}_s \\ & + \{-8 + [-8 + (-4h^2 - 4)\text{Ma}^2]\text{Pe}_s^2 - 8\text{Ma}\text{Pe}_s h\}[\cosh(h)]^2 \\ & - 8[2\text{Pe}_s^2h + \text{Ma}(h^2 + 1)\text{Pe}_s + 2h]\sinh(h)\cosh(h) \\ & + [2(h^2 + 1)^2\text{Ma}^2 + 8h^2]\text{Pe}_s^2 + 8h\text{Ma}(h^2 + 1)\text{Pe}_s + 8h^2 \end{aligned} \right]}. \quad (\text{A15})$$

APPENDIX B: VALIDATION OF RESULTS

In this section, we verify the expression for the velocity of a sheet near a surfactant-laden interface by comparing it with similar expressions derived in the literature for several special cases. For instance, when a sheet is far away from the interface, its velocity should be the same as the sheet's velocity in an unbounded fluid [26]:

$$\lim_{h \rightarrow \infty} U_2 = \frac{1}{2}(-\tilde{a}^2 - \tilde{d}^2 + \tilde{b}^2 + 2\tilde{a}\tilde{b}). \quad (\text{B1})$$

As $\lambda \rightarrow \infty$ or $\text{Ma} \rightarrow \infty$, the sheet's velocity should approach the velocity of a sheet placed symmetrically between two plane walls [3].

$$\begin{aligned} \lim_{\lambda \rightarrow \infty} U_2 &= \lim_{\text{Ma} \rightarrow \infty} U_2 \\ &= \frac{((\tilde{a}^2 - \tilde{b}^2 + \tilde{d}^2)[\cosh(h)]^2 - 2\cosh(h)\sinh(h)\tilde{a}\tilde{b} + (-h^2 - 1)\tilde{a}^2 + 2\tilde{a}\tilde{b}h + (-h^2 + 1)\tilde{b}^2 - \tilde{d}^2(h^2 + 1))}{2h^2 - 2[\cosh(h)]^2 + 2}. \end{aligned} \quad (\text{B2})$$

It is obvious that a surfactant-laden interface behaves as a rigid wall in the limit $\lambda \rightarrow \infty$ but such a behavior in the limit $\text{Ma} \rightarrow \infty$ requires some explanation. As $\text{Ma} \rightarrow \infty$, the surfactant becomes incompressible [10,58], i.e., $O(1)$ changes in interfacial tension are caused by infinitesimal changes in the surfactant concentration. So, treating Γ as constant, the surfactant transport equation simplifies to $\frac{\partial}{\partial x}(u|_{y=h}) = 0$. The only

solution of this equation that enables the velocity of fluid 2 to approach the negative of the sheet's velocity, far away from the interface, is $u|_{y=h} = -U$. The sheet near an interface with such interface boundary conditions ($u|_{y=h} = -U$, $v|_{y=h} = 0$) is essentially equivalent to a sheet near a plane wall.

In the limit $\text{Ma} \rightarrow 0$ or $\text{Pe}_s \rightarrow 0$, the sheet's velocity should approach its velocity near a plane clean interface. This

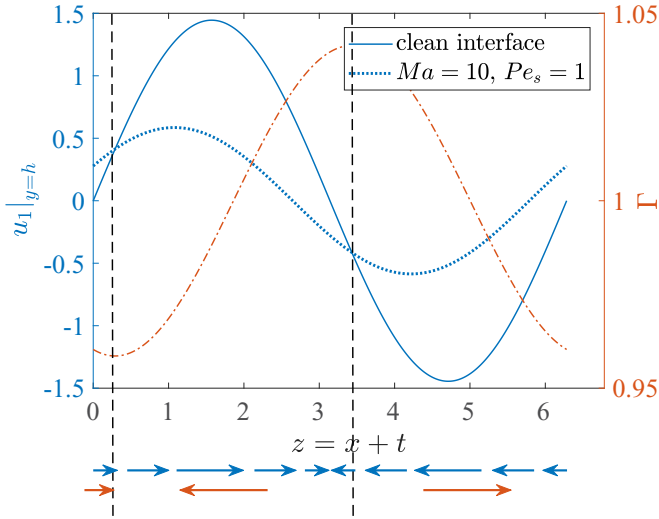


FIG. 7. Comparison of interface slip of a clean interface (blue solid line) with that of a surfactant-laden interface (blue dotted line). Also plotted is the surfactant concentration on the surfactant-laden interface (red dash-dotted line). The vertical dashed lines are just for reference. The blue (upper) and red (lower) arrows denote, respectively, the vector field of clean interface slip and the direction of Marangoni induced slip. The axis for the interface slip is on the left while that for surfactant concentration is on the right. Here, $Ma = 10$ and $Pe_s = 1$ for the surfactant-laden interface. Also, $\epsilon = 0.1$ is used to calculate Γ while the values of the other parameters $h, \lambda, a,$ and d are kept the same as those of Fig. 3.

velocity was derived for a sheet passing transverse waves in the positive x direction (Taylor’s sheet) [4]. As we considered the sheet passing transverse waves in the negative x direction, its velocity near a plane surfactant-laden interface in the limits $Ma \rightarrow 0$ or $Pe_s \rightarrow 0$ should approach the negative of Taylor’s

swimming sheet velocity near a plane clean interface.

$$\begin{aligned} & \lim_{Ma, \tilde{a}, \tilde{d} \rightarrow 0} U_2 \\ &= \lim_{Pe_s, \tilde{a}, \tilde{d} \rightarrow 0} U_2 \\ &= \frac{\tilde{b}^2}{2} \frac{\tilde{b}^2 h (h\lambda + 1)}{h^2 \lambda - [\cosh(h)]^2 \lambda - \sinh(h) \cosh(h) + h + \lambda}. \end{aligned} \tag{B3}$$

APPENDIX C: EFFECT OF SURFACTANT REDISTRIBUTION ON THE INTERFACE SLIP

In this section, we analyze the influence of surfactant redistribution on the leading order interface slip when a sheet passing transverse waves is located near an interface. Let us first discuss how the viscosity ratio of an interface affects the interface slip and the swimming velocity for a sheet near a plane clean interface. We plot these features for a sheet passing transverse waves near a plane clean interface in Fig. 6. We observe that the interface slip decreases while the swimming velocity increases with an increase in the viscosity ratio of a clean interface. As an increase in the viscosity ratio corresponds to an increase in the viscosity of fluid above the interface (for a fixed viscosity of fluid below the interface), such high viscosity fluid above the interface hinders the interface slip.

When a sheet is near a clean interface, the interface slip varies in a sinusoidal fashion with the x coordinate, i.e., $u_{1|y=h} = A \sin(x + t + \phi)$, where A and ϕ are the amplitude and phase of the slip, respectively [see blue solid line in Fig. 7; vector field of the interface slip is shown by blue (upper) arrows in this figure]. When we compare slip (such as slip of clean and surfactant-laden interface or slip of a surfactant-laden interface at various values of Ma or Pe_s), we are essentially comparing the amplitude of the sinusoidal

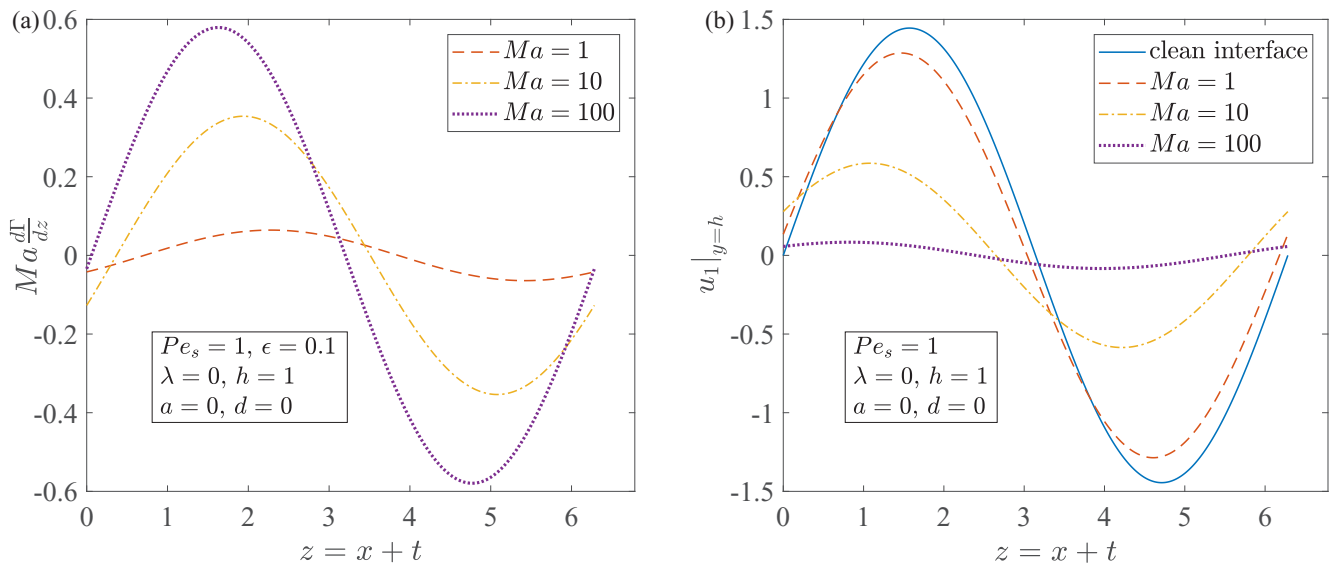


FIG. 8. The variation of (a) the Marangoni stress and (b) the leading order interface slip with the Marangoni number Ma for a fixed surface Péclet number $Pe_s = 1$. Here $\epsilon = 0.1$ is used to calculate the Marangoni stresses while the values of the other parameters $\lambda, h, a,$ and d are kept the same as those of Fig. 3.

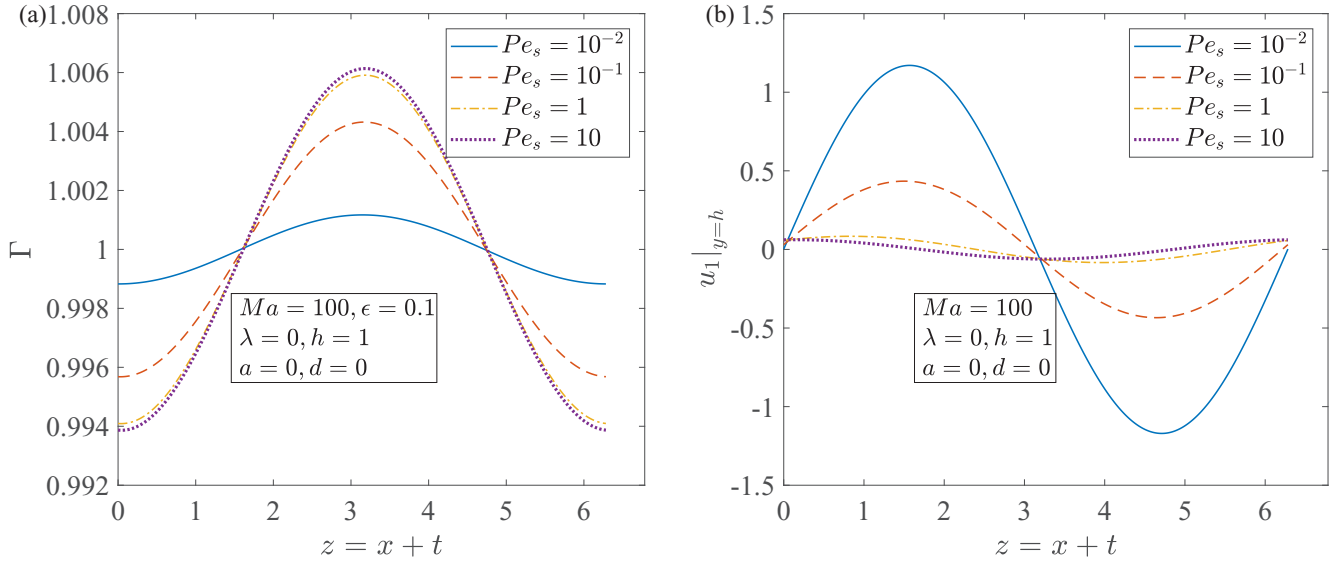


FIG. 9. The variation of (a) the surfactant concentration and (b) the leading order interface slip with the surface Péclet number Pe_s , for a fixed Marangoni number $Ma = 100$. Here $\epsilon = 0.1$ is used to calculate surfactant concentration while the values of the other parameters λ , h , a , and d are kept the same as those of Fig. 3.

functions. Now, if a sheet is near a surfactant-laden interface, the surfactant concentration varies nonmonotonically with the position, as shown by red dash-dotted lines in Fig. 7. As the interfacial tension decreases with an increase in the surfactant concentration, this nonhomogeneous surfactant concentration gives rise to a nonhomogeneous interfacial tension which in turn causes the tensile stress imbalance on the interface, pulling the fluid from the regions of maximum Γ toward the regions of minimum Γ . This Marangoni induced slip velocity is shown by red (lower) arrows in Fig. 7. The slip of a surfactant-laden interface is the sum of the slip of a clean

interface and the Marangoni induced slip. As this Marangoni induced slip is directed oppositely to the clean interface's slip at most of the locations, the slip of a surfactant-laden interface is less than the slip of a clean interface (see the blue dotted line in Fig. 7 for the slip of a surfactant-laden interface).

With an increase in Ma , the Marangoni stresses increase [see Fig. 8(a)] which in turn reduce the slip of an interface [see Fig. 8(b)]. At large Ma like $Ma = 100$, with an increase in Pe_s the advective transport of surfactant increases in comparison to its diffusive transport; this increases the gradients in the surfactant concentration [see Fig. 9(a)] or Marangoni

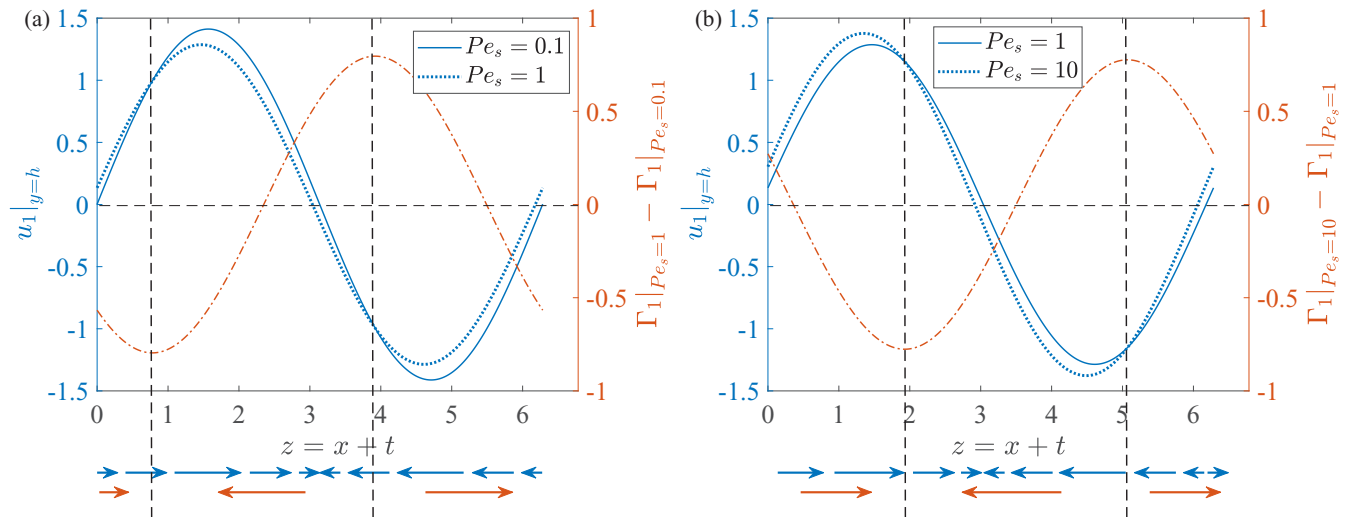


FIG. 10. Comparison of the interface slip of surfactant-laden interfaces with different Pe_s but with a fixed $Ma = 1$. In each plot, the interface slip at low and high Pe_s are denoted, respectively, by blue solid and blue dotted lines. Also plotted is the change in the surfactant concentration at high Pe_s , in comparison to that at low Pe_s , (red dash-dotted line). The dashed lines are just for reference. In (a) the low and high Pe_s are 0.1 and 1, while in (b) they are 1 and 10, respectively. The blue (upper) and red (lower) arrows denote, respectively, the vector field of the surfactant-laden interface's slip at low Pe_s and the direction of the Marangoni induced slip as Pe_s is increased from its low to high value. The axis for the interface slip is on the left while that for the change in the surfactant concentration is on the right. The values of the other parameters h , λ , a , and d are kept the same as those of Fig. 3.

stresses which in turn reduce the interface slip [see Fig. 9(b)]. For these values of Ma and Pe_s at which the interface slip decreases with an increase in Ma for a fixed Pe_s (or with an increase in Pe_s for a fixed Ma), the swimming velocity increases with the corresponding variation of Ma or Pe_s (see Fig. 3).

We note that the Marangoni stresses increase with an increase in Pe_s at any fixed Ma , not just at large Ma . But at small Ma , with an increase in Pe_s , the increasing Marangoni stresses reduce the interface slip during the initial increase of Pe_s [see Fig. 10(a)] while they increase the interface slip during the

latter increase of Pe_s [see Fig. 10(b)]. This is expected because during the initial (respectively, latter) increase in Pe_s , the Marangoni induced slip is directed opposite to (respectively, along) the slip of a relatively clean interface at most of the interface locations. Compare the red (lower) arrows with the blue (upper) arrows in Fig. 10 to understand this observation. Here relatively clean interface is an interface with lower Pe_s . At this value of Ma at which the interface slip varies non-monotonically with an increase in Pe_s , the swimming velocity also varies non-monotonically with an increase in Pe_s [see Fig. 3(b)].

-
- [1] N. Desai and A. M. Ardekani, Modeling of active swimmer suspensions and their interactions with the environment, *Soft Matter* **13**, 6033 (2017).
- [2] A. J. Reynolds, The swimming of minute organisms, *J. Fluid Mech.* **23**, 241 (1965).
- [3] D. F. Katz, On the propulsion of micro-organisms near solid boundaries, *J. Fluid Mech.* **64**, 33 (1974).
- [4] Y. Man and E. Lauga, Phase-separation models for swimming enhancement in complex fluids, *Phys. Rev. E* **92**, 023004 (2015).
- [5] S. Wang and A. M. Ardekani, Swimming of a model ciliate near an air-liquid interface, *Phys. Rev. E* **87**, 063010 (2013).
- [6] E. Lauga, W. R. DiLuzio, G. M. Whitesides, and H. A. Stone, Swimming in circles: Motion of bacteria near solid boundaries, *Biophys. J.* **90**, 400 (2006).
- [7] R. Di Leonardo, D. Dell'Arciprete, L. Angelani, and V. Iebba, Swimming With an Image, *Phys. Rev. Lett.* **106**, 038101 (2011).
- [8] A. P. Berke, L. Turner, H. C. Berg, and E. Lauga, Hydrodynamic Attraction of Swimming Microorganisms by Surfaces, *Phys. Rev. Lett.* **101**, 038102 (2008).
- [9] D. Lopez and E. Lauga, Dynamics of swimming bacteria at complex interfaces, *Phys. Fluids* **26**, 071902 (2014).
- [10] V. A. Shaik and A. M. Ardekani, Point force singularities outside a drop covered with an incompressible surfactant: Image systems and their applications, *Phys. Rev. Fluids* **2**, 113606 (2017).
- [11] N. Desai, V. A. Shaik, and A. M. Ardekani, Hydrodynamics-mediated trapping of micro-swimmers near drops, *Soft Matter* **14**, 264 (2018).
- [12] S. Lee, J. W. M. Bush, A. E. Hosoi, and E. Lauga, Crawling beneath the free surface: Water snail locomotion, *Phys. Fluids* **20**, 082106 (2008).
- [13] D. Crowdy, S. Lee, O. Samson, E. Lauga, and A. E. Hosoi, A two-dimensional model of low-Reynolds number swimming beneath a free surface, *J. Fluid Mech.* **681**, 24 (2011).
- [14] V. A. Shaik and A. M. Ardekani, Motion of a model swimmer near a weakly deforming interface, *J. Fluid Mech.* **824**, 42 (2017).
- [15] S. Wang and A. Ardekani, Inertial squirmer, *Phys. Fluids* **24**, 101902 (2012).
- [16] G. Li, A. Ostace, and A. M. Ardekani, Hydrodynamic interaction of swimming organisms in an inertial regime, *Phys. Rev. E* **94**, 053104 (2016).
- [17] G. J. Li, A. Karimi, and A. M. Ardekani, Effect of solid boundaries on swimming dynamics of microorganisms in a viscoelastic fluid, *Rheol. Acta* **53**, 911 (2014).
- [18] G. Li and A. M. Ardekani, Collective Motion of Microorganisms in a Viscoelastic Fluid, *Phys. Rev. Lett.* **117**, 118001 (2016).
- [19] G. Li and A. M. Ardekani, Near wall motion of undulatory swimmers in non-Newtonian fluids, *Eur. J. Comput. Mech.* **26**, 44 (2017).
- [20] V. A. Shaik, V. Vasani, and A. M. Ardekani, Locomotion inside a surfactant-laden drop at low surface Péclet numbers, *J. Fluid Mech.* **851**, 187 (2018).
- [21] M. Sickert and F. Rondelez, Shear Viscosity of Langmuir Monolayers in the Low-Density Limit, *Phys. Rev. Lett.* **90**, 126104 (2003).
- [22] T. M. Fischer, Comment on "Shear Viscosity of Langmuir Monolayers in the Low-Density Limit," *Phys. Rev. Lett.* **92**, 139603 (2004).
- [23] M. Sickert, F. Rondelez, and H. A. Stone, Single-particle Brownian dynamics for characterizing the rheology of fluid Langmuir monolayers, *Europhys. Lett.* **79**, 66005 (2007).
- [24] J. R. Samaniuk and J. Vermant, Micro and macrorheology at fluid-fluid interfaces, *Soft Matter* **10**, 7023 (2014).
- [25] G. Taylor, Analysis of the swimming of microscopic organisms, *Proc. R. Soc. London, Ser. A* **209**, 447 (1951).
- [26] J. R. Blake, Infinite models for ciliary propulsion, *J. Fluid Mech.* **49**, 209 (1971).
- [27] T. K. Chaudhury, On swimming in a visco-elastic liquid, *J. Fluid Mech.* **95**, 189 (1979).
- [28] L. D. Sturges, Motion induced by a waving plate, *J. Non-Newtonian Fluid Mech.* **8**, 357 (1981).
- [29] E. Lauga, Propulsion in a viscoelastic fluid, *Phys. Fluids* **19**, 083104 (2007).
- [30] J. R. Vélez-Cordero and E. Lauga, Waving transport and propulsion in a generalized Newtonian fluid, *J. Non-Newtonian Fluid Mech.* **199**, 37 (2013).
- [31] E. E. Riley and E. Lauga, Enhanced active swimming in viscoelastic fluids, *Europhys. Lett.* **108**, 34003 (2014).
- [32] G. Li and A. M. Ardekani, Undulatory swimming in non-Newtonian fluids, *J. Fluid Mech.* **784**, R4 (2015).
- [33] G. J. Elfring and G. Goyal, The effect of gait on swimming in viscoelastic fluids, *J. Non-Newtonian Fluid Mech.* **234**, 8 (2016).
- [34] D. R. Hewitt and N. J. Balmforth, Taylor's swimming sheet in a yield-stress fluid, *J. Fluid Mech.* **828**, 33 (2017).
- [35] A. M. Leshansky, Enhanced low-Reynolds-number propulsion in heterogeneous viscous environments, *Phys. Rev. E* **80**, 051911 (2009).

- [36] H. C. Fu, V. B. Shenoy, and T. R. Powers, Low-Reynolds-number swimming in gels, *Europhys. Lett.* **91**, 24002 (2010).
- [37] M. S. Krieger, M. A. Dias, and T. R. Powers, Minimal model for transient swimming in a liquid crystal, *Eur. Phys. J. E* **38**, 94 (2015).
- [38] A. M. Siddiqui and A. R. Ansari, An analysis of the swimming problem of a singly flagellated microorganism in a fluid flowing through a porous medium, *J. Porous Media* **6**, 235 (2003).
- [39] W. Shack and T. Lardner, A long wavelength solution for a microorganism swimming in a channel, *Bull. Math. Biol.* **36**, 435 (1974).
- [40] R. E. Smelser, W. J. Shack, and T. J. Lardner, The swimming of spermatozoa in an active channel, *J. Biomechanics* **7**, 349 (1974).
- [41] J. B. Shukla, B. R. P. Rao, and R. S. Parihar, Swimming of spermatozoa in cervix: Effects of dynamical interaction and peripheral layer viscosity, *J. Biomechanics* **11**, 15 (1978).
- [42] J. B. Shukla, P. Chandra, R. Sharma, and G. Radhakrishnamacharya, Effects of peristaltic and longitudinal wave motion of the channel wall on movement of micro-organisms: Application to spermatozoa transport, *J. Biomechanics* **21**, 947 (1988).
- [43] M. A. Dias and T. R. Powers, Swimming near deformable membranes at low Reynolds number, *Phys. Fluids* **25**, 101901 (2013).
- [44] S. A. Mirbagheri and H. C. Fu, *Helicobacter pylori* Couples Motility and Diffusion to Actively Create a Heterogeneous Complex Medium in Gastric Mucus, *Phys. Rev. Lett.* **116**, 198101 (2016).
- [45] T. R. Ives and A. Morozov, The mechanism of propulsion of a model microswimmer in a viscoelastic fluid next to a solid boundary, *Phys. Fluids* **29**, 121612 (2017).
- [46] E. O. Tuck, A note on a swimming problem, *J. Fluid Mech.* **31**, 305 (1968).
- [47] S. Childress, *Mechanics of Swimming and Flying* (Cambridge University Press, Cambridge, 1981).
- [48] S. Childress, Inertial swimming as a singular perturbation, in *ASME 2008 Dynamic Systems and Control Conference, Parts A and B* (ASME, New York, 2008), pp. 1413–1420.
- [49] O. S. Pak and E. Lauga, The transient swimming of a waving sheet, *Proc. R. Soc. London, Ser. A* **466**, 107 (2010).
- [50] A. Sokolov, I. S. Aranson, J. O. Kessler, and R. E. Goldstein, Concentration Dependence of the Collective Dynamics of Swimming Bacteria, *Phys. Rev. Lett.* **98**, 158102 (2007).
- [51] A. Sokolov, R. E. Goldstein, F. I. Feldchtein, and I. S. Aranson, Enhanced mixing and spatial instability in concentrated bacterial suspensions, *Phys. Rev. E* **80**, 031903 (2009).
- [52] A. Sokolov and I. S. Aranson, Reduction of Viscosity in Suspension of Swimming Bacteria, *Phys. Rev. Lett.* **103**, 148101 (2009).
- [53] A. W. Adamson and A. P. Gast, *Physical Chemistry of Surfaces*, 6th ed. (Wiley, New York, 1997).
- [54] D. J. Smith, E. A. Gaffney, H. Gadêlha, N. Kapur, and J. C. Kirkman-Brown, Bend propagation in the flagella of migrating human sperm, and its modulation by viscosity, *Cell Motil. Cytoskeleton* **66**, 220 (2009).
- [55] C.-H. Chang and E. I. Franses, Adsorption dynamics of surfactants at the air/water interface: A critical review of mathematical models, data, and mechanisms, *Colloids Surf., A* **100**, 1 (1995).
- [56] S. Wang, T. Guo, S. Dabiri, P. P. Vlachos, and A. M. Ardekani, Effect of surfactant on bubble collisions on a free surface, *Phys. Rev. Fluids* **2**, 043601 (2017).
- [57] D. S. Valkovska and K. D. Danov, Determination of bulk and surface diffusion coefficients from experimental data for thin liquid film drainage, *J. Colloid Interface Sci.* **223**, 314 (2000).
- [58] J. Bławdziewicz, V. Cristini, and M. Loewenberg, Stokes flow in the presence of a planar interface covered with incompressible surfactant, *Phys. Fluids* **11**, 251 (1999).
- [59] C. Datt, L. Zhu, G. J. Elfring, and O. S. Pak, Squirming through shear-thinning fluids, *J. Fluid Mech.* **784**, R1 (2015).